Inorg. Chem. **2007**, *46*, 1727–1736

Mechanism of $[\gamma\text{-}H_2SiV_2W_{10}O_{40}]^{4-}$-Catalyzed Epoxidation of Alkenes with Hydrogen Peroxide

Yoshinao Nakagawa[†] and Noritaka Mizuno*[,†,‡]

Department of Applied Chemistry, School of Engineering, The University of Tokyo, 7-3-1 Hongo, Bunkyo-ku, Tokyo 113-8656, Japan, and Core Research for Evolutional Science and Technology, Japan Science and Technology Agency, 4-1-8 Honcho, Kawaguchi, Saitama 332-0012, Japan

Received December 6, 2006

The mechanism of $[\gamma\text{-}H_2SiV_2W_{10}O_{40}]^{4-}$-catalyzed epoxidation of alkenes with hydrogen peroxide in acetonitrile/*tert*-butyl alcohol was investigated. The negative Hammett ρ^+ (–0.88) for the competitive oxidation of p-substituted styrenes and the low X_{SO} (X_{SO} = (nucleophilic oxidation)/(total oxidation)) value of <0.01 for the $[\gamma\text{-}H_2SiV_2W_{10}O_{40}]^{4-}$-catalyzed oxidation of thianthrene-5-oxide reveal that the strong electrophilic oxidant species is formed on $[\gamma\text{-}H_2SiV_2W_{10}O_{40}]^{4-}$ (**I**). The preferable formation of *trans*-epoxide for the epoxidation of 3-substituted cyclohexenes shows the steric constraints of the active oxidant on **I**. The ^{51}V NMR, ^{183}W NMR, and CSI–MS spectroscopy show that the reaction of **I** with hydrogen peroxide leads to the reversible formation of a hydroperoxo species $[\gamma\text{-}HSiV_2W_{10}O_{39}OOH]^{4-}$ (**II**). The successive dehydration of **II** forms **III**, which possibly has an active oxygen species of a $\mu\text{-}\eta^2\text{:}\eta^2$-peroxo group. The kinetic and spectroscopic studies show that the present epoxidation proceeds via **III**. The energy diagram of the epoxidation with density functional theory (DFT) supports the idea.

Introduction

Epoxidation of alkenes has received considerable academic and industrial interests because epoxides are widely used as epoxy resins, paints, surfactants, and intermediates in various organic syntheses.[1] The use of hydrogen peroxide as a terminal oxidant for the catalytic epoxidation system produces only water as a byproduct.[2] Many catalytic systems with high-valent early transition metals such as titanium(IV), tungsten(VI), and rhenium(VII) have been reported to be effective for the epoxidation of alkenes with hydrogen peroxide.[3]

Vanadium(V) compounds are not generally effective catalysts for the epoxidation of nonfunctionalized alkenes with hydrogen peroxide because of the contribution of the radical mechanism,[4] while the vanadium-catalyzed epoxidation with organic hydroperoxides[5] and the oxidation of halogen ions with hydrogen peroxide by vanadium-containing enzymes (vanadium haloperoxidases) are well-known.[6]

Recently, the catalytic activity of polyoxometalates has received much attention because of the feasible design of catalytically active sites and because the redox and acidic properties can be controlled at atomic or molecular levels.[7] Various lacunary or transition-metal-substituted polyoxometalates have been reported to be active for the catalytic

* To whom correspondence should be addressed. E-mail: tmizuno@mail.ecc.u-tokyo.ac.jp. Tel: +81-3-5841-7272. Fax: +81-3-5841-7220.
† The University of Tokyo.
‡ Japan Science and Technology Agency.

(1) Sheldon, R. A.; Kochi, J. K. *Metal-Catalyzed Oxidations of Organic Compounds*; Academic Press: New York, 1981.
(2) Lane, B. S.; Burgess, K. *Chem. Rev.* **2003**, *103*, 2457.
(3) (a) Grigoropoulou, G.; Clark, J. H.; Elings, J. A. *Green Chem.* **2003**, *5*, 1. (b) Noyori, R.; Aoki, M.; Sato, K. *Chem. Commun.* **2003**, 1977. (c) Arends, I. W. C. E.; Sheldon, R. A. *Top. Catal.* **2002**, *19*, 133.
(4) (a) Wei, D.; Chuei, W.; Haller, G. L. *Catal. Today* **1999**, *51*, *501*. (b) Schuchardt, U.; Guerreiro, M. C.; Shul'pin, G. B. *Russ. Chem. Bull.* **1998**, *47*, 247. (c) Neumann, R.; Levin-Elad, M. *Appl. Catal,. A* **1995**, *122*, *85*. (d) Bellussi, G.; Rigutto, M. S. *Stud. Surf. Sci. Catal.* **1994**, *85*, 177. (e) Bortolini, O.; Di Furia, F.; Scrimin, P.; Modena, G. *J. Mol. Catal.* **1980**, *7*, 59. (f) Eisenbraun, E. J.; Bader, A. R.; Polacheck, J. W.; Reif, E. *J. Org. Chem.* **1963**, *28*, 2057.
(5) (a) Bolm, C. *Coord. Chem. Rev.* **2003**, *237*, 245. (b) Conte, V.; Di Furia, F.; Licini, G. *Appl. Catal., A* **1997**, *157*, 335.
(6) (a) Crans, D. C.; Smee, J. J.; Gaidamauskas, E.; Yang, L. *Chem. Rev.* **2004**, *104*, 849. (b) Rehder, D. *Inorg. Chem. Commun.* **2003**, *6*, 604. (c) Butler, A. *Coord. Chem. Rev.* **1999**, *187*, 17. (d) Butler, A.; Walker, J. V. *Chem. Rev.* **1993**, *93*, 1937.
(7) (a) Hill, C. L. In *Comprehensive Coordination Chemistry II*; McCleverty, J. A., Meyer, T. J., Eds.; Elsevier: Amsterdam, The Netherlands, 2003; Vol. 4, p 679. (b) Kozhevnikov, I. V. *Catalysis by Polyoxometalates*; John Wiley & Sons, Ltd: Chichester, England, 2002. (c) Kozhevnikov, I. V. *Chem. Rev.* **1998**, *98*, 171. (d) Mizuno, N.; Misono, M. *Chem. Rev.* **1998**, *98*, 199. (e) Neumann, R. *Prog. Inorg. Chem.* **1998**, *47*, 317. (f) Okuhara, T.; Mizuno, N.; Misono, M. *Adv. Catal.* **1996**, *41*, 113. (g) Hill, C. L.; Prosser-McCartha, C. M. *Coord. Chem. Rev.* **1995**, *143*, 407.

10.1021/ic0623258 CCC: $37.00 © 2007 American Chemical Society
Published on Web 01/20/2007

epoxidation.[8] The steric effects of the active oxidants formed on the bulky polyoxometalates have also been reported in some cases.[9]

The mechanism of vanadium-based oxidation with peroxides has extensively been studied. For the vanadium-catalyzed epoxidation with organic hydroperoxides, it has been accepted that the oxygen transfer reaction to an alkene proceeds via an intermediate with asymmetric η^2-coordination of the alkylperoxide to the Lewis acid vanadium center.[10] Allylic alcohols are epoxidized more rapidly than NDunfunctionalized alkenes, which is explained by the rapid coordination of the hydroxyl group to the vanadium center followed by the intramolecular oxygen transfer.[11] For the oxidation of halogen ions and sulfides with hydrogen peroxide by vanadium haloperoxidases and their mimics, the formation of a hydroperoxovanadium species has been proposed based on kinetic and NMR results.[12,13] It is proposed that the protonation of a symmetric η^2-peroxovanadium complex provides a nucleophilic center like that of the asymmetric alkylperoxovanadium species, while catalytically active hydroperoxovanadium complexes have never been isolated. Butler et al. reported that the divanadium complex $V_2O_2(O_2)_3$ was an active species for the oxidation of bromide with hydrogen peroxide, while the mononuclear ions of $VO(O_2)^+$ and $VO(O_2)_2^-$ were inactive.[14]

We have previously reported the epoxidation of alkenes with hydrogen peroxide catalyzed by divanadium-substituted polyoxotungstate [γ-$H_2SiV_2W_{10}O_{40}$]$^{4-}$ in acetonitrile (MeCN)/*tert*-butyl alcohol (*t*-BuOH) (v/v = 1/1) (entries 1−11, 13, 17, and 19−23 in Table 1).[15] Nonactivated aliphatic terminal C_3−C_{10} alkenes including propene could be oxidized to the corresponding epoxide with ≥99% selectivity and ≥87% efficiency of H_2O_2 utilization (entries 1−5). The epoxidation of *cis*- and *trans*-2-octenes gave *cis*-2,3-epoxyoctane (90% yield) and *trans*-2,3-epoxyoctane (6% yield), respectively (entries 6 and 7). The configuration around the C=C moieties was retained in these epoxides. Acid-sensitive styrene was epoxidized to give 1,2-epoxy styrene as the sole product (entry 13). This system requires only one equivalent of hydrogen peroxide with respect to the alkene and produces the epoxide with high yield, stereospecificity, diastereoselectivity, and regioselectivity.[15c] While the formation of hydroperoxo species [γ-$HSiV_2W_{10}O_{39}(OOH)$]$^{4-}$ by the reaction of **I** with H_2O_2 in 1,2-dichloroethane has been shown by NMR and mass spectroscopy,[15a] the whole mechanism of **I**-catalyzed epoxidation in the most effective solvent of MeCN/*t*-BuOH is still unclear. In this paper, we investigate the detailed mechanism of the **I**-catalyzed epoxidation of alkenes with hydrogen peroxide.

Table 1. Epoxidation of Various Alkenes Catalyzed by **I**[a]

entry	substrate	yield of epoxide %	selectivity to epoxide %	H_2O_2 efficiency %
1[b]	propene	87	99	87
2[c]	1-butene	91	99	91
3	1-hexene	92	99	92
4	1-octene	93	99	93
5	1-decene	93	99	93
6	*cis*-2-octene	90	99[d]	90
7	*trans*-2-octene	6	99[e]	6
8	2-methyl-1-heptene	88	98	90
9	2-methyl-2-heptene	27	99	27
10	cyclohexene	90	99	92
11	cyclooctene	93	99	93
12[f]	cyclododecene	71	99[f]	71
13	styrene	88	99	88
14	7-octen-1-ol	79	99	79
15	1-octen-3-ol	95	97[g]	95
16	1-hepten-4-ol	94	99[h]	94
17	3-methylcyclohexene	91	97[i]	91
18	3-ethylcyclohexene	91	99[j]	91
19	2-cyclohexen-1-ol	87	95[k]	91
20	*trans*-1,4-hexadiene	91	99[l]	91
21	(*R*)-(+)-limonene	90	95[m]	91
22	1-methyl-1,4-cyclohexadiene	76	89[n]	90
23	7-methyl-1,6-octadiene	83	99[o]	87

[a] Conditions: MeCN (1.5 mL), *t*-BuOH (1.5 mL), **I** (5 μmol, 1.7 mM), substrate (0.1 mmol, 33 mM), H_2O_2 (30% aq, 0.1 mmol, 33 mM), 293 K, 24 h. H_2O_2 efficiency (%) = products (mol)/consumed H_2O_2 (mol) × 100. [b] Propene (6 atm). [c] 1-Butene (3 atm). [d] Only *cis*-epoxide. [e] Only *trans*-epoxide. [f] Substrate: cis/trans = 70/30 (5/95 after the reaction). Epoxide: cis/trans = 96/4. [g] Epoxy alcohol: threo/erythro = 80/20. [h] Epoxy alcohol: {(2*R*,4*R*) + (2*S*,4*S*)}/{(2*S*,4*R*) + (2*R*,4*S*)} = 58/42. [i] Epoxide: cis/trans = 5/95. [j] Epoxide: cis/trans = 4/96. [k] Epoxide: cis/trans = 12/88. 2-Cyclohexen-1-one (select. 5%) was formed as a byproduct. [l] Ratio of 1,2-epoxide to total epoxide was 0.99. [m] Ratio of 8,9-epoxide to total epoxide was 0.99. [n] Ratio of 4,5-epoxide to total epoxide was 0.88. Toluene (select. 11%) was formed as a byproduct. [o] Ratio of 1,2-epoxide to total epoxide was 0.93.

Experimental Section

Instruments. IR spectra were measured on Jasco FT/IR-460 Plus using KBr disks. NMR spectra were recorded at 298 K (unless noted) on a JEOL JNM-EX-270 (^{29}Si, 53.45 MHz; ^{183}W, 11.20 MHz; ^{51}V, 70.90 MHz; ^{17}O, 36.5 MHz) spectrometer. Chemical shifts (δ) of ^{29}Si, ^{183}W, ^{51}V, and ^{17}O were reported in parts per million downfield from external $SiMe_4$ (solvent, $CDCl_3$), Na_2WO_4 (solvent, D_2O), $VOCl_3$ (neat), and H_2O (neat), respectively. UV−vis spectra were recorded on a PerkinElmer Lambda 12 spectrometer. Cold-spray ionization mass (CSI−MS) spectra were recorded

(8) Kamata, K.; Yonehara, K.; Sumida, Y.; Yamaguchi, K.; Hikichi, S.; Mizuno, N. *Science* **2003**, *300*, 964.

(9) (a) Kamata, K.; Nakagawa, Y.; Yamaguchi, K.; Mizuno, N. *J. Catal.* **2004**, *224*, 224. (b) Neumann, R.; Juwiler, D. *Tetrahedron* **1996**, *52*, 8781. (c) Mizuno, N.; Tateishi, M.; Hirose, T.; Iwamoto, M. *Chem. Lett.* **1993**, 1985. (d) Mansuy, D.; Bartoli, J.-F.; Battioi, P.; Lyon, D. K.; Finke, R. G. *J. Am. Chem. Soc.* **1991**, *113*, 7222.

(10) (a) Deubel, D. V.; Frenking, G.; Gisdakis, P.; Hermann, W. A.; Rösch, N.; Sundermeyer, J. *Acc. Chem. Res.* **2004**, *37*, 645. (b) Talsi, E. P.; Chinakov, V. D.; Babenko, V. P.; Zamaraev, K. I. *J. Mol. Catal.* **1993**, *81*, 235. (c) Mimoun, H.; Mignard, M.; Brechot, P.; Saussine, L. *J. Am. Chem. Soc.* **1986**, *108*, 3711.

(11) (a) Hoveyda, A. H.; Evans, D. A.; Fu, G. C. *Chem. Rev.* **1993**, *93*, 1307. (b) Chong, A. O.; Sharpless, K. B. *J. Org. Chem.* **1977**, *42*, 1587.

(12) (a) Smith, T. S.; Pecoraro, V. L. *Inorg. Chem.* **2002**, *41*, 6754. (b) Časný, M.; Rehder, D. *Chem. Commun.* **2001**, 921.

(13) Conte, V.; Bortolini, O.; Carraio, M.; Moro, S. *J. Inorg. Biochem.* **2000**, *80*, 41.

(14) Clague, M. J.; Butler. A. *J. Am. Chem. Soc.* **1995**, *117*, 3475.

(15) (a) Nakagawa, Y.; Kamata, K.; Kotani, M.; Yamaguchi, K.; Mizuno, N. *Angew. Chem., Int. Ed.* **2005**, *44*, 5136. (b) Mizuno, N.; Nakagawa, Y.; Yamaguchi, K. *J. Mol. Catal. A: Chem.* **2006**, *251*, 286. (c) After the previous two reports (refs 15a and 15b), we have found that the oxidation of alkenols (entries 14−16 in Table 1) selectively gave the corresponding epoxides (≥95%) with the OH groups intact, as follows:

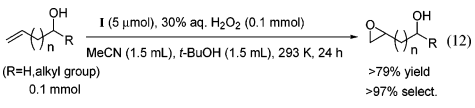

(12)

on a JEOL JMS-T100LC. Typical measurement conditions were as follows: olifice voltage (−95 V), sample flow (0.05 mL min^{-1}), concentration (0.14 mM), spray temp (253 K), and ion source temp (room temp). The spectroscopic measurements were carried out with the tetra-*n*-butylammonium salt of **I**, unless otherwise stated. GC analyses were performed on a Shimadzu GC-14B with a flame ionization detector equipped with a TC-WAX capillary (internal diameter = 0.25 mm, length = 30 m) or a SE-30 packed column. Mass spectra were recorded on a Shimadzu GCMS-QP2010 at an ionization voltage of 70 eV equipped with a DB-WAX capillary column (internal diameter = 0.25 mm, length = 30 m).

Synthesis and Characterization of $[(n\text{-}C_4H_9)_4N]_4[\gamma\text{-}H_2SiV_2W_{10}O_{40}]\cdot H_2O$. An aqueous solution of $[\gamma\text{-}H_2SiV_2W_{10}O_{40}]^{4-}$ was prepared according to ref 16, and the anion was isolated as the tetra-*n*-butylammonium (TBA) salt. The potassium salt of $[\gamma\text{-}SiW_{10}O_{36}]^{8-}$ ($K_8[\gamma\text{-}SiW_{10}O_{36}]\cdot 12H_2O$,[17] 8 g, 2.7 mmol) was quickly dissolved in 1 M HCl (28 mL) followed by the addition of $NaVO_3$ (0.5 M, 11 mL, 5.5 mmol). The mixture was gently stirred for 5 min. The solution was filtered off followed by the addition of $[(n\text{-}C_4H_9)_4N]Br$ (8 g, 25 mmol) in a single step. The resulting yellow precipitate was collected by the filtration and then washed with an excess amount of water (300 mL). The crude product was purified twice with the precipitation method (addition of 1 L of H_2O into an acetonitrile solution of the tetra-*n*-butylammonium salt of **I** (50 mL)). The analytically pure tetra-*n*-butylammonium salt of **I** was obtained as a pale-yellow powder. Yield: 7.43 g (76%). Anal. Calcd for $[(C_4H_9)_4N]_4H_2SiV_2W_{10}O_{40}\cdot H_2O$: C, 21.4; H, 4.15; N, 1.56; Si, 0.78; V, 2.83; W, 51.1; H_2O, 0.50. Found: C, 21.4; H, 3.91; N, 1.59; Si, 0.79; V, 2.88; W, 51.2; H_2O, 0.50. ^{51}V NMR (MeCN): δ −564 ppm ($\Delta\nu_{1/2}$ = 130 Hz). ^{183}W NMR (MeCN-d_3): δ −82.2 ppm ($\Delta\nu_{1/2}$ = 9.6 Hz), −95.6 ppm ($\Delta\nu_{1/2}$ = 2.5 Hz), and −129.7 ppm ($\Delta\nu_{1/2}$ = 2.9 Hz) with an integrated intensity ratio of 1.9:1.0:2.1. ^{29}Si NMR (MeCN-d_3): δ −84.0 ppm ($\Delta\nu_{1/2}$ = 2.0 Hz). ^1H NMR (MeCN-d_3): δ 5.07 (2H, s, V−O*H*−V), 3.13 (cation), 1.63 (cation), 1.43 (cation), 0.99 ppm (cation). The UV−vis spectrum (in MeCN) showed shoulder bands at 240 (ϵ = 36 000 M^{-1} cm^{-1}), 285 (24 000), and 350 nm (5900). IR (KBr, cm^{-1}): 1151(w), 1106(w), 1057(w), 1004(m), 995(m), 966(s), 915(vs), 904-(vs), 875(s), 840(m), 790(vs), 691(m), 550(m), 519(w), 482(w), 457(w), 405(m). The tetra-*n*-butylammonium salt of **I** was used for the experiments, unless otherwise stated.

Catalytic Reactions. The typical reaction experiment was conducted as follows: **I** (5 μmol), MeCN (anhydrous (H_2O, <0.005%), 1.5 mL), *t*-BuOH (recrystallized, 1.5 mL), oxidant (30% aqueous H_2O_2, 100 μmol), and substrates (100 μmol) were charged in the reaction vessel. The reaction was carried out at 293 ± 0.2 K. The reaction solution was periodically sampled and analyzed by GC in combination with mass spectroscopy. The products were identified by the comparison of mass and NMR spectra with those of authentic samples. The carbon balance in each experiment was in the range of 95−100%. The reaction rates were determined with the reaction profiles at the low conversion (≤10%) of H_2O_2. The H_2O_2 remaining after the reaction was analyzed by the $Ce^{4+/3+}$ titration.[18] The products for the oxidation of thianthrene-5-oxide were quantitatively analyzed by HPLC according to ref 19. The reaction conditions (i.e., concentration of substrate, substrate to oxidant ratio, reaction temperature, etc.) were controlled to minimize overoxidation to trioxide for the evolution of the true electronic nature of the oxidant.[19d]

(16) Canny, J.; Thouvenot, R.; Tézé, A.; Hervé, G.; Leparulo-Loftus, M.; Pope, M. T. *Inorg. Chem.* **1991**, *30*, 976.
(17) Tézé, A.; Hervé, G. *Inorg. Synth.* **1990**, *27*, 85.

Table 2. Epoxidation of 1-Octene Catalyzed by **I** in Various Solvents[a]

entry	solvent	initial rate mM h^{-1}	yield of epoxide %	conv. of H_2O_2 %
1	MeCN/*t*-BuOH (v/v = 1/1)	23	93	>99
2	MeCN/*t*-AmOH (v/v = 1/1)	5.1	76	97
3	MeCN/3-methyl-3-pentanol (v/v =1/1)	2.1	41	88
4	MeCN/*i*-PrOH (v/v = 1/1)	14	47[b]	>99
5	MeCN/*sec*-BuOH (v/v = 1/1)	5.8	33[c]	>99
6	MeCN/MeOH (v/v = 1/1)	<0.01	1	14
7	MeCN/EtOH (v/v = 1/1)	<0.01	2	9
8	MeCN/benzene (v/v = 1/1)	0.1	8	82
9	MeCN	0.2	7	89
10	1,2-dichloroethane	0.8	7	>99
11[d]	1,2-dichloroethane/*t*-BuOH (v/v = 1/1)	18	93	>99
12	acetone	<0.01	<1	14
13	MeCN/*t*-BuOH (v/v = 5/1)		85	>99
14	MeCN/*t*-BuOH (v/v = 2/1)		86	>99
15	MeCN/*t*-BuOH (v/v = 1/2)		93	>99

[a] Conditions: solvent (3 mL), **I** (5 μmol, 1.7 mM), 1-octene (0.1 mmol, 33 mM), H_2O_2 (30% aq, 0.1 mmol, 33 mM), 293 K, 24 h. [b] Acetone (40% based on H_2O_2) was formed. [c] 2-Butanone (37% based on H_2O_2) was formed. [d] The tetra-*n*-decylammonium salt of **I** was used as a catalyst because of the low solubility of the tetra-*n*-butylammonium salt.

Quantum Chemical Calculations. The calculations were carried out at the B3LYP level theory[20] with 6-31++G** basis sets for H, C, and O atoms, 6-31G* for Si atoms, and the double-ζ quality basis sets with effective core potentials proposed by Hay and Wadt[21] for V and W atoms. The geometries were optimized within the following symmetry restrictions: D_{2h} for ethene; C_{2v} for H_2O, epoxyethane, $[\gamma\text{-}H_2SiV_2W_{10}O_{40}]^{4-}$, $[\gamma\text{-}SiV_2W_{10}O_{38}(O_2)]^{4-}$, and $[\gamma\text{-}SiV_2W_{10}O_{39}]^{4-}$; no symmetry restrictions for dimethyldioxirane, peracetic acid, $[\gamma\text{-}HSiV_2W_{10}O_{39}(OOH)]^{4-}$, and all transition states. Transition state structures were searched by numerically estimating the matrix of second-order energy derivatives at every optimization step and by requiring exactly one eigenvalue of this matrix to be negative. For the transition states, the frequency analysis was conducted at the same level without diffuse and polarization functions at the final geometry. The optimized geometries were shown in Tables S1−S6 (Supporting Information). The zero-point vibrational energies were not included. All calculations were performed with the Gaussian03 program package.[22]

Results and Discussion

Effects of Solvents. Table 2 shows the **I**-catalyzed epoxidation of 1-octene in various solvents. The catalyst **I** was almost inactive in MeCN, 1,2-dichloroethane, and acetone. The epoxidation proceeded in the mixed solvents containing secondary or tertiary alcohols (entries 1−5 and 11). Among

(18) Vogel, A. I. *A Textbook of Quantitative Inorganic Analysis Including Elementary Instrumental Analysis*; Longman: New York, 1978.
(19) (a) Sato, K.; Hyodo, M.; Aoki, M.; Zheng, X. Q.; Noyori, R. *Tetrahedron* **2001**, *57*, 2469. (b) Adam, W.; Mithcell, C. M.; Saha-Möller, C. R.; Selvam, T.; Weichold, O. *J. Mol. Catal. A: Chem.* **2000**, *154*, 251. (c) Adam, W.; Golsch, D. *J. Org. Chem.* **1997**, *62*, 115. (d) Adam, W.; Golsch, D.; Görth, F. C. *Chem.−Eur. J.* **1996**, *2*, 255. (e) Bonchio, M.; Conte, V.; Assunta, M.; Conciliis, D.; Di Furia, F.; Ballistrei, F. P.; Tomaselli, G. A.; Toscano, R. M. *J. Org. Chem.* **1995**, *60*, 4475. (f) Herrman, W. A.; Fischer, R. W.; Correia, J. D. G. *J. Mol. Catal.* **1994**, *94*, 213. (g) Adam, W.; Golsch, D. *Chem. Ber.* **1994**, *127*, 1111.
(20) Becke, A. D. *J. Chem. Phys.* **1993**, *98*, 1372.
(21) Hay, P. J.; Wadt, W. R. *J. Chem. Phys.* **1985**, *82*, 270.

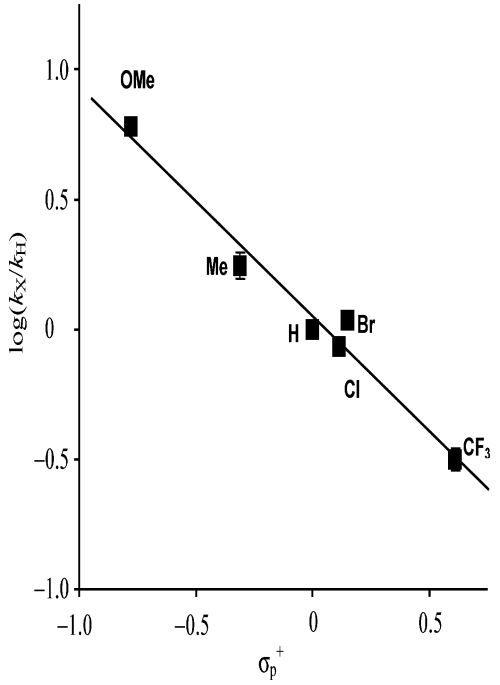

Figure 1. Hammett plots ($\log(k_X/k_H)$ vs σ_p plots) for competitive oxidation of styrene and p-substituted styrenes. Reaction conditions: Styrene (0.2 mmol), p-substituted styrene (0.2 mmol), **I** (10 μmol), H_2O_2 (30% aq, 0.2 mmol), MeCN/*t*-BuOH (v/v = 1, 6 mL), 293 K. Slope = −0.88.

the solvents used, a mixed solvent of MeCN and *t*-BuOH around the 1:1 (v/v) ratio gave the highest yield, while the oxidation of secondary alcohols simultaneously proceeded in the mixed solvents with secondary alcohols. The epoxidation did not proceed in the mixed solvents with primary alcohols (entries 6 and 7). The epoxidation with tert-butylhydroperoxide (TBHP) did not proceed in both MeCN and MeCN/*t*-BuOH (v/v = 1).

Electronic and Steric Character of the Active Oxygen Species. The good linearity of Hammett plots ($\log(k_X/k_H)$ versus σ^+) for the competitive oxidation of styrene and p-substituted styrenes (Figure 1) suggests that the present epoxidation proceeds via a single mechanism. The negative ρ^+ value of −0.88 agrees with the formation of an electrophilic oxidant on **I**.[23]

The electronic character of the active oxygen species formed on **I** was further examined with thianthrene-5-oxide (SSO), which has been used as a probe to examine the electronic character of an oxidant; electrophilic oxidants

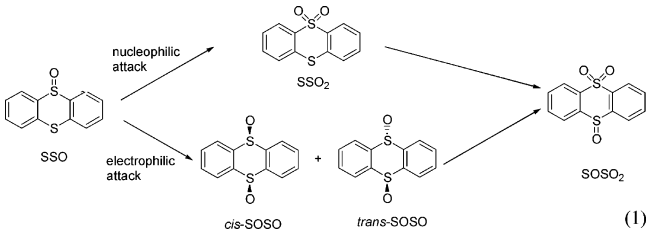

(1)

predominantly attack the sulfide site of SSO to form the diastereomeric *cis*- and *trans*-thianthrene-5,10-dioxides (SOSO), while nucleophilic ones attack the sulfoxide site of SSO to form thianthrene-5,5-dioxide (SSO_2) (eq 1).[19]

The results for oxidation of SSO by **I** showed the extremely low X_{SO} value (X_{SO} = (nucleophilic oxidation)/(total oxidation) = (SSO_2 + $SOSO_2$)/(SSO_2 + SOSO + 2$SOSO_2$); $SOSO_2$ = thianthrene-5,5,10-trioxide) of <0.01 (eq 2), indicating the strong electrophilic nature of the active oxygen species.[24]

$$\underset{(200\ \mu\text{mol})}{\text{SSO}} \xrightarrow[\text{MeCN (4 mL), } t\text{-BuOH (1 mL), 293 K, 8 h}]{\mathbf{I}\ (2\ \mu\text{mol}),\ 30\%\ \text{aq}\ H_2O_2\ (50\ \mu\text{mol})} \underset{\substack{(49\ \mu\text{mol})\\ >99\%\ \text{select}}}{\textit{trans}\text{-SOSO}} + \underset{\text{(trace)}}{\textit{cis}\text{-SOSO}} + \underset{\text{(trace)}}{SSO_2} + \underset{\text{(trace)}}{SOSO_2} \quad (2)$$

The 3-alkyl-substituted cyclohexenes provide a quantitative measure of purely steric effects for the epoxidations since electronic interactions between the C=C double bond and the allylic substituents are not possible.[25] The epoxidation of 3-alkyl-substituted cyclohexenes (entries 17 and 18 in Table 1) gave the corresponding epoxides with the oxirane ring trans to the substituents and was highly diastereoselective; the trans diastereoselectivity (trans/cis = 95/5) for the epoxidation of 3-methyl-1-cyclohexene by **I** (eq 3) was higher than those of titanosilicates (92/8),[25] methyltrioxorhenium (49/51),[26] and stoichiometric oxidants of *m*-CPBA (48/52)[27] and dimethyldioxirane (52/48).[28]

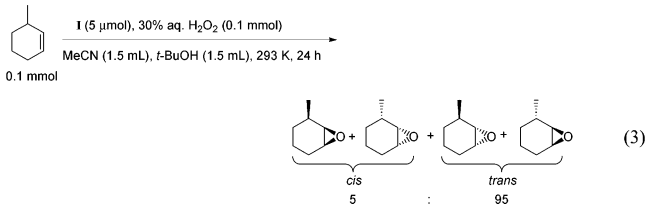

(3)

Further, it is noted that more accessible, but less nucleophilic, double bonds in nonconjugated dienes such as *trans*-

(22) Frisch, M. J.; Trucks, G. W.; Schlegel, H. B.; Scuseria, G. E.; Robb, M. A.; Cheeseman, J. R.; Montgomery, J. A., Jr.; Vreven, T.; Kudin, K. N.; Burant, J. C.; Millam, J. M.; Iyengar, S. S.; Tomasi, J.; Barone, V.; Mennucci, B.; Cossi, M.; Scalmani, G.; Rega, N.; Petersson, G. A.; Nakatsuji, H.; Hada, M.; Ehara, M.; Toyota, K.; Fukuda, R.; Hasegawa, J.; Ishida, M.; Nakajima, T.; Honda, Y.; Kitao, O.; Nakai, H.; Klene, M.; Li, X.; Knox, J. E.; Hratchian, H. P.; Cross, J. B.; Bakken, V.; Adamo, C.; Jaramillo, J.; Gomperts, R.; Stratmann, R. E.; Yazyev, O.; Austin, A. J.; Cammi, R.; Pomelli, C.; Ochterski, J. W.; Ayala, P. Y.; Morokuma, K.; Voth, G. A.; Salvador, P.; Dannenberg, J. J.; Zakrzewski, V. G.; Dapprich, S.; Daniels, A. D.; Strain, M. C.; Farkas, O.; Malick, D. K.; Rabuck, A. D.; Raghavachari, K.; Foresman, J. B.; Ortiz, J. V.; Cui, Q.; Baboul, A. G.; Clifford, S.; Cioslowski, J.; Stefanov, B. B.; Liu, G.; Liashenko, A.; Piskorz, P.; Komaromi, I.; Martin, R. L.; Fox, D. J.; Keith, T.; Al-Laham, M. A.; Peng, C. Y.; Nanayakkara, A.; Challacombe, M.; Gill, P. M. W.; Johnson, B.; Chen, W.; Wong, M. W.; Gonzalez, C.; Pople, J. A. *Gaussian 03*, revision B.03; Gaussian, Inc.: Wallingford, CT, 2004.

(23) (a) Liu, C.-J.; Yu, W.-Y.; Li, S.-G.; Che, C.-M. *J. Org. Chem.* **1998**, *63*, 7364. (b) Al-Ajlouni, A. M.; Espenson, J. H. *J. Am. Chem. Soc.* **1995**, *117*, 9243. (c) Baumstark, A. L.; Vasquez, P. C. *J. Org. Chem.* **1988**, *53*, 3437. (d) Hanzlik, R. P.; Shearer, G. O. *J. Am. Chem. Soc.* **1975**, *97*, 5231.

(24) The high trans/cis ratio of SOSO can be explained by the steric effect; the sterically hindered active species encumber attack of the *cis*-sulfide lone pair by the *peri*-hydrogen atoms of SSO.[19c]

(25) Adam, W.; Corma, A.; García, H.; Weichold, O. *J. Catal.* **2000**, *196*, 339.

(26) Adam, W.; Mitchell, C. M.; Saha-Möller, C. R. *Eur. J. Org. Chem.* **1999**, 785.

(27) Bellucci, G.; Berti, G.; Ferreti, M.; Igrosso, G.; Mastrorilli, E. *J. Org. Chem.* **1978**, *43*, 422.

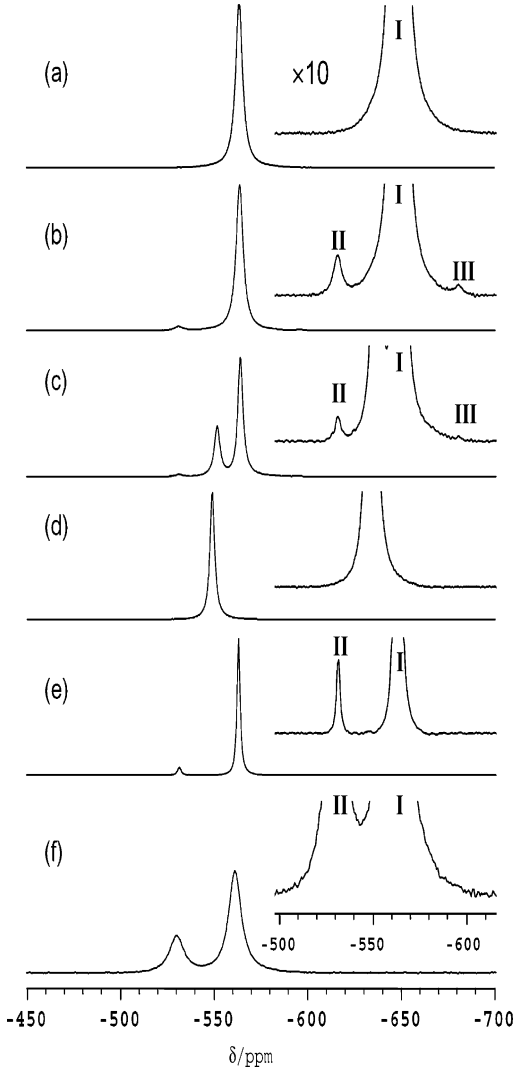

Figure 2. ^{51}V NMR spectra of (a) **I** (3.3 mM) in MeCN/*t*-BuOH (v/v = 1/1) and that treated with 10 equiv of H_2O_2 (30% aq, 33 mM) for 1.5 min at 293 K in (b) MeCN/t-BuOH (v/v = 1/1), (c) MeCN/*i*-PrOH (v/v = 1/1), (d) MeCN/MeOH (v/v = 1/1), (e) MeCN, and (f) 1,2-$C_2H_4Cl_2$.

1,4-hexadiene, (*R*)-(+)-limonene, 7-methyl-1,6-octadiene, and 1-methyl-1,4-cyclohexadiene were highly regioselectively epoxidized in high yields (entries 20−23 in Table 1). The ratios of [less-substituted epoxide]/[total epoxides] (≥0.88) were much higher than those reported for the other epoxidation systems.[9a,29] The reactivity order of a series of C_8−alkenes[30] and the specific regioselectivity for epoxidation of nonconjugated dienes probably reflects the electronic and steric characters.[9a]

These results for the competitive oxidation of p-substituted styrenes, oxidation of SSO, and oxygenation of 3-substituted cyclohexenes, the reactivity order of a series of C_8−alkenes, and regioselectivity for epoxidation of nonconjugated dienes show that the strong electrophilic oxidant species with strong steric hindrance is formed by the reaction of **I** with hydrogen peroxide.

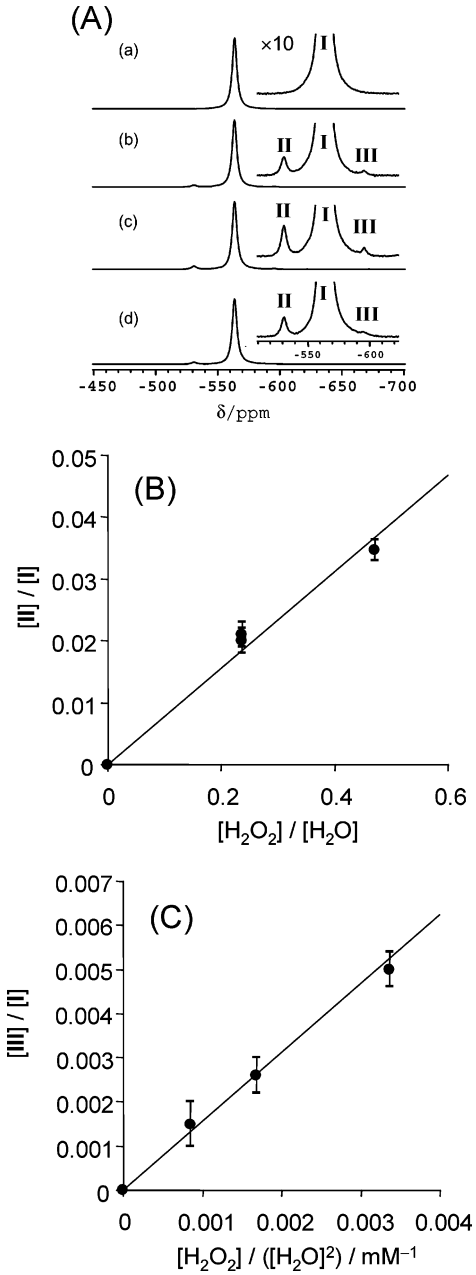

Figure 3. Changes in (B) [**II**] and (C) [**III**] with [H_2O_2] and [H_2O]. (A) ^{51}V NMR spectra of (a) **I** (3.3 mM) in MeCN/*t*-BuOH (v/v = 1/1) and (b−d) **I** (3.3 mM) treated with 10−20 equiv of H_2O_2 (33−66 mM) and 42−84 equiv of H_2O (140−280 mM) at 293 K for 1.5 min. (b) H_2O_2 (33 mM), H_2O (140 mM). (c) H_2O_2 (66 mM), H_2O (140 mM). (d) H_2O_2 (66 mM), H_2O (280 mM). (B) The dependence of the concentration of **II** on those of H_2O and H_2O_2.

(28) Murray, R. W.; Singh, M.; Williams, B. L.; Moncrieff, H. M. *J. Org. Chem.* **1996**, *61*, 1830.

(29) (a) Lai, T.; Lee, S. K.; Yeung, L.; Liu, H.; Williams, I. D.; Chang, C. K. *Chem. Commun.* **2003**, 620. (b) Bhyrappa, P.; Young, J. K.; Moore, J. S.; Suslick, K. S. *J. Am. Chem. Soc.* **1996**, *118*, 5708. (c) Suslick, K. S.; Cook, B. R. *J. Chem. Soc., Chem. Commun.* **1987**, 200.

(30) The relative reactivity (rate) of a series of C_8−alkenes decreased in the order of 2-methyl-1-heptene (1.1) > 1-octene (1.0 taken as unity) > *cis*-2-octene (0.87) > 2-methyl-2-heptene (0.03) > *trans*-2-octene (<0.01). Moreover, for the competitive epoxidation of *cis*- and *trans*-2-octenes (100 μmol of each, the other conditions were the same as those in Table 1), the initial rates were 0.32 and <0.001 mM min^{-1}, respectively. The ratio of the formation rate of *cis*-2,3-epoxyoctane to that of the *trans*-isomer was more than 3×10^2 and is much higher than those (1.3−11.5) reported for the other stereospecific epoxidation systems.[8] The yields of *cis*-2,3-epoxyoctane and the *trans*-isomer (based on H_2O_2) even after 24 h were 91 and 2%, respectively.[15]

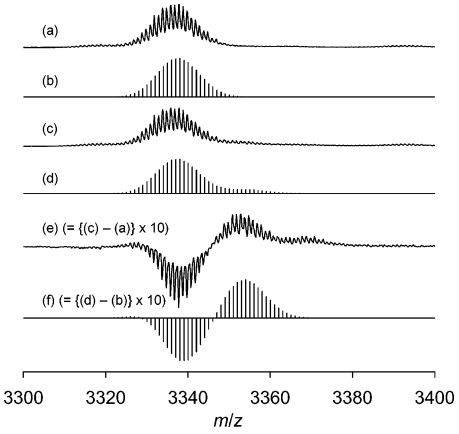

Figure 4. CSI−MS spectra (anion mode, *m*/*z* 3300−3400) of **I** (0.14 mM) (a) as-synthesized and (c) treated with 240 equiv of H_2O_2 (95% aq) in MeCN/*t*-BuOH (v/v = 1/1) for 3 min at room temperature. (b) The lines calculated for $[(TBA)_3H_2SiV_2W_{10}O_{40}]^-$. (d) The lines calculated for a mixture of $[(TBA)_3H_2SiV_2W_{10}O_{40}]^-$ (80%), $[(TBA)_3HSiV_2W_{10}O_{39}(OOH)]^-$ (10%), and $[(TBA)_3SiV_2W_{10}O_{40}]^-$ (10%). (e) The spectrum (a) was subtracted from the spectrum (c). (f) The spectrum (b) was subtracted from the spectrum (d).

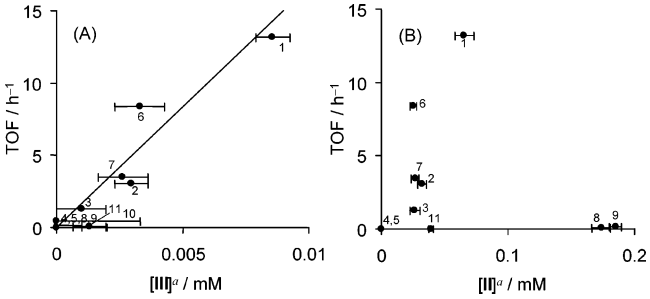

Figure 5. Dependences of epoxidation of rates on (A) [**II**] and (B) [**III**] in various solvents. *a*The [**II**] and [**III**] were estimated by (the initial concentration of **I**) × (the ratio of the respective signal intensities to the sum of the vanadium signal intensities). Conditions for epoxidation: **I** (1.67 mM), 1-octene (33 mM), H_2O_2 (30% aq, 33 mM), 293 K. The ^{51}V NMR measurements of **II** and **III** were carried out under the following conditions: **I** (3.3 mM), H_2O_2 (30% aq, 33 mM), room temperature. The numbers show the solvents used for the epoxidation: 1 (MeCN/*t*-BuOH), 2 (MeCN/*t*-AmOH), 3 (MeCN/3-methyl-3-pentanol), 4 (MeCN/MeOH), 5 (MeCN/EtOH), 6 (MeCN/*i*-PrOH), 7 (MeCN/*sec*-BuOH), 8 (MeCN/benzene), 9 (MeCN), 10 (1,2-dichloroethane), 11 (acetone).

Reaction of I with H_2O_2. We have reported the formation of $[\gamma\text{-}SiV_2W_{10}O_{38}(\mu\text{-}OH)(\mu\text{-}OOH)]^{4-}$ (**II**) with the C_s symmetry by the reaction of **I** with H_2O_2 in 1,2-dichloroethane (eq 4) on the basis of the following results.[15a] The polyoxometalate **II** showed one ^{51}V NMR signal at −530 ppm, six ^{183}W NMR signals at −79, −83, −92, −104, −127, and −132 ppm with the intensity ratio of 2:2:1:1:2:2, respectively, two ^{1}H NMR signals at 5.10 and 9.45 ppm with the intensity ratio of 1:1, respectively, and the cold-spray ionization mass (CSI−MS, anion mode) signals centered at *m*/*z* 3354 (Figures S1−S4).[31]

$$[\gamma\text{-}H_2SiV_2W_{10}O_{40}]^{4-}\ (\mathbf{I}) + H_2O_2 \rightleftharpoons [\gamma\text{-}SiV_2W_{10}O_{38}(\mu\text{-}OH)(\mu\text{-}OOH)]^{4-}\ (\mathbf{II}) + H_2O \quad (4)$$

The reactivity of **I** with H_2O_2 as well as the catalytic activity of **I** (Table 2) much depended upon the solvents. Figure 2 shows the ^{51}V NMR spectra of **I** treated with 10 equiv of hydrogen peroxide (30% aq) at 293 K in various solvents. Upon the addition of 10 equiv of H_2O_2 with respect to **I**, each signal intensity reached a constant value within 1 min, and the sum of the signal intensities was unchanged. In neat MeCN and 1,2-dichloroethane, in which the catalytic reaction hardly proceeded, two signals of **I** and **II** were observed (Figure 2e and 2f). In MeCN/*t*-BuOH (v/v = 1/1), in which **I** showed the highest activity, a new signal at −595 ppm (**III**) was observed in addition to the two signals (Figure 2b). In MeCN/MeOH, only one signal at −549 ppm, assignable to the monomethylester $[HSiV_2W_{10}O_{39}(\mu\text{-}OMe)]^{4-}$,[32] was observed. In MeCN/*i*-PrOH, two signals of **I** and the monoisopropylester (−552 ppm)[32] were observed in addition to two weak signals of **II** and **III**.

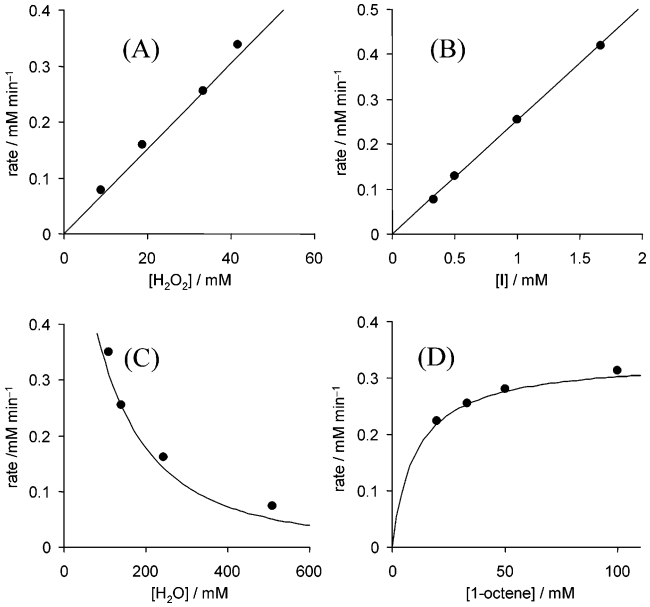

Figure 6. Dependences of epoxidation rates on (A) $[H_2O_2]$, (B) [**I**], (C) $[H_2O]$, and (D) [1-octene] in MeCN/*t*-BuOH (v/v = 1) at 293 K. Lines were calculated with eq 11. (A) **I** (1 mM), 1-octene (33 mM), H_2O_2 (10−40% aq, 8.9−42 mM), H_2O (140 mM); (B) **I** (0.33−1.7 mM), 1-octene (33 mM), H_2O_2 (33 mM), H_2O (140 mM); (C) **I** (1 mM), 1-octene (33 mM), H_2O_2 (33 mM), H_2O (110−510 mM); (D) **I** (1 mM), 1-octene (20−100 mM), H_2O_2 (33 mM), H_2O (140 mM).

Chart 1. Proposed Structure of the Vanadium Center in **III**

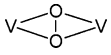

Scheme 1. Proposed Mechanism for the Epoxidation Catalyzed by **I**

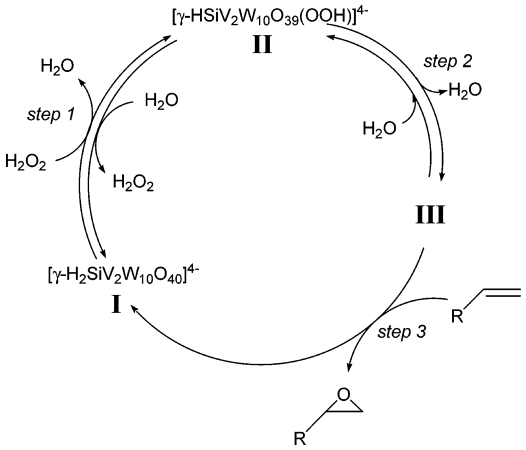

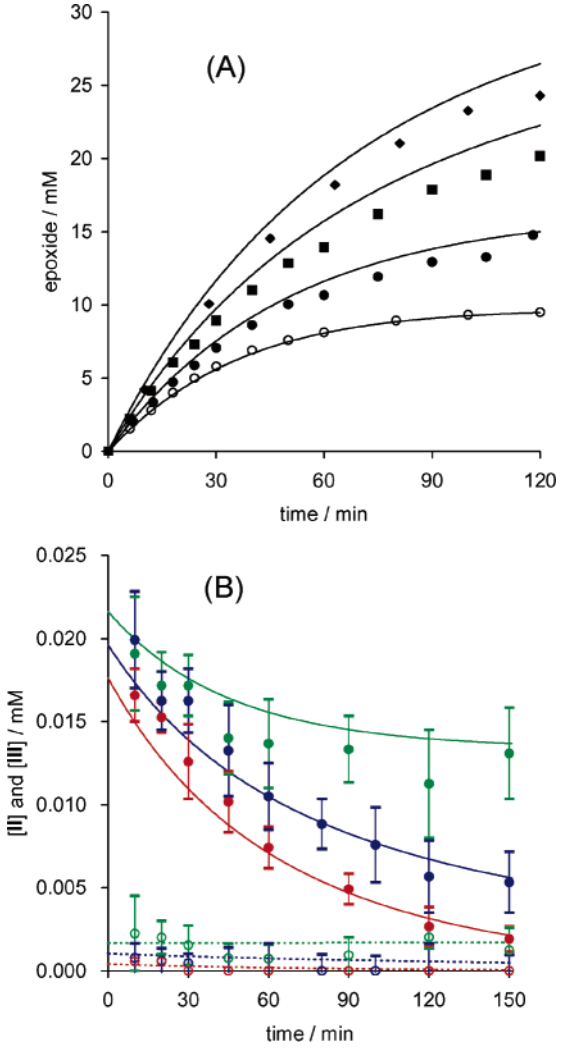

Figure 7. Changes in (A) epoxide yields and (B) [**II**] (closed circles) and [**III**] (open circles) for epoxidation of 1-octene catalyzed by **I** as a function of time. Solid and dotted lines in (A) and (B) were calculated with eqs 6−11. (A) Conditions: 1-octene (10 mM (○), 16.7 mM (●), 33.3 mM (■), 100 mM (♦)), **I** (5 μmol), H_2O_2 (30% aq, 100 μmol), MeCN (1.5 mL), *t*-BuOH (1.5 mL), 293 K. Yields are based on H_2O_2. (B) Conditions: 1-octene (16.7 mM (green), 33.3 mM (blue), 100 mM (red)), **I** (5 μmol), H_2O_2 (30% aq, 100 μmol), MeCN (1.5 mL), *t*-BuOH (1.5 mL), 293 K.

Figure 3 shows the effects of H_2O_2 and H_2O on the formation of **II** and **III**. The ratio of the concentration of **II** ([**II**]) to that of **I** ([**I**]) was proportional to $[H_2O_2]/[H_2O]$, supporting the reversible formation of **II** (eq 4). The ratio of the concentration of **III** ([**III**]) to [**I**] was proportional to $[H_2O_2]/[H_2O]^2$, suggesting the successive dehydration of **II** to form **III**, as shown in eq 5. The same dependences of [**II**]/[**I**] and [**III**]/[**I**] on $[H_2O_2]$ and $[H_2O]$ were observed in MeCN.

$$\mathbf{II} \rightleftharpoons \mathbf{III} + H_2O \qquad (5)$$

The CSI−MS spectrum of **I** in MeCN/*t*-BuOH showed the most intense parent ion peaks centered at *m*/*z* 3338 with the isotopic distribution that agreed with the calculated pattern of $[(TBA)_3H_2SiV_2W_{10}O_{40}]^-$ (Figures 4a,b and S5). Upon the addition of 240 equiv of H_2O_2 (95% aq, 33 mM), new weak peaks centered at *m*/*z* 3354 appeared, and the parent ion peaks were slightly shifted to the lower *m*/*z* values (Figure 4c and 4e). The ^{51}V NMR spectra showed that the treatment of **I** with 10 equiv of H_2O_2 (95% aq, 33 mM) in MeCN/*t*-BuOH gave a mixture of **I**, **II**, and **III** with the ratio of 80:10:10, respectively (Figure S6). On the basis of the ^{51}V NMR data, the pattern calculated for a mixture of $[(TBA)_3H_2SiV_2W_{10}O_{40}]^-$ (80%), $[(TBA)_3HSiV_2W_{10}O_{39}(OOH)]^-$ (10%), and $[(TBA)_3SiV_2W_{10}O_{40}]^-$ (10%) is shown in Figure 4d and well reproduced Figure 4c.

The two vanadium atoms in **III** would be equivalent because only one ^{51}V NMR signal was observed for **III**. In addition, **III** is formed by the dehydration of **II**. Therefore, the μ-η^2:η^2-peroxo group is a possible active oxygen species. The μ-η^2:η^2-peroxo bridge has been reported for dicopper complexes.[33,34]

Kinetics and Mechanism. Upon the addition of 1-octene (10 equiv) to a MeCN/*t*-BuOH (v/v = 1/1) solution of **I** (3.3 mM) treated with 10 equiv of H_2O_2 (30% aqueous solution), the ^{51}V NMR signal of **II** was weakened and that of **III** almost disappeared (Figures 2b and S7). The dependences of epoxidation rates on [**II**] and [**III**] in various solvents are shown in Figure 5. The rate increased with increase in [**III**] (Figure 5A), while no correlation between the rate and [**II**] was observed (Figure 5B). These facts suggest that the reaction of **III** with 1-octene is rapid and that **III** plays an important role in the **I**-catalyzed epoxidation.

No induction period was observed for the epoxidation by **I**. The kinetic studies on the epoxidation of 1-octene showed the first-order dependences of the reaction rate on the concentrations of hydrogen peroxide ($[H_2O_2]$, 8.9−42 mM, Figure 6A) and **I** (0.33−1.7 mM, Figure 6B). The rate decreased with the increase in the concentration of water

(31) We conducted ^{17}O NMR experiments to detect hydroperoxo species **II** formed by the reaction of **I** with ^{17}O-labeled H_2O_2 (80% enriched; purchased from Icon as a 2% solution in $H_2{}^{16}O$ and concentrated to 30% at a reduced pressure). While the formation of **II** was confirmed with the ^{51}V NMR spectrum, no ^{17}O NMR signals assignable to **II** were observed in the range of −1000 to +2000 ppm. The ^{17}O NMR spectrum of the solution of **I** treated with $H_2{}^{17}O$ showed the broad signal of V−(*O*H)$_2$−V in **I** around +120 ppm ($\Delta\nu_{1/2}$ = 3 kHz at room temperature). It has been reported that the ^{17}O NMR signals of peroxo and alkylperoxo species are sometimes too broad to be observed (see Postel, M.; Brevard, C.; Arzoumanian, H.; Riess, J. G. *J. Am. Chem. Soc.* **1983**, *105*, 4922 and Groarke, M.; Gonçalves, I. S.; Herrman, W. A.; Kühn, F. E. *J. Organomet. Chem.* **2002**, *649*, 108). Căsny et al. reported the ^{17}O NMR signals and the tentative assignment of hydroperoxovanadium species formed by the treatment of *Ascophyllum nodosum* bromoperoxidase with ^{17}O-enriched H_2O_2 (Căsny, M.; Rehder, D.; Schmidt, H.; Vilter, H.; Conte, V. *J. Inorg. Biochem.* **2000**, *80*, 157). Therefore, the detection of the ^{17}O NMR signals of hydroperoxo groups bound to early transition metals such as Ti, Mo, and V has been very difficult. On the other hand, the ^1H NMR spectrum was more informative; by labeling of the peroxidic oxygens with $H_2{}^{17}O_2$, the ^1H NMR signal at 9.5 ppm was significantly broadened from $\Delta\nu_{1/2}$ = 1.2 to 6.4 Hz (in MeCN-d_3 at 273 K), while the line width of the signal at 5.1 ppm was not changed ($\Delta\nu_{1/2}$ = 1.4 ± 0.1 Hz). This strongly suggests that the proton of the signal at 9.5 ppm is bound to the peroxidic oxygen, supporting the assignment of the signal as a hydroperoxo group.

(32) (a) Nakagawa, Y.; Uehara, K.; Mizuno, N. *Inorg. Chem.* **2005**, *44*, 14. (b) Nakagawa, Y.; Uehara, K.; Mizuno, N. *Inorg. Chem.* **2005**, *44*, 9068.

(33) (a) Mirica, L. M.; Ottenwaelder, X.; Stack, T. D. P. *Chem. Rev.* **2004**, *104*, 1013. (b) Que, L., Jr.; Tolman, W. B. *Angew. Chem., Int. Ed.* **2002**, *41*, 1114.

(34) The detection of **III** with IR, Raman, and UV−vis spectra has been unsuccessful because of the overlap of the strong bands of the polyoxometalate framework.

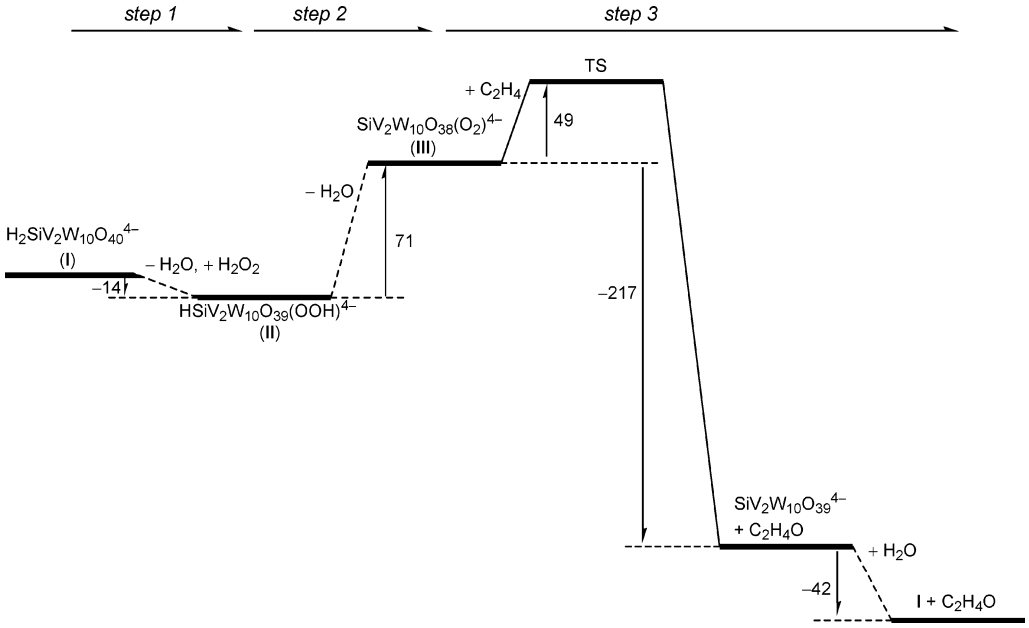

Figure 8. Calculated energy diagram of the epoxidation of ethene catalyzed by **I** in the gas phase (energies in kJ mol^{-1}).

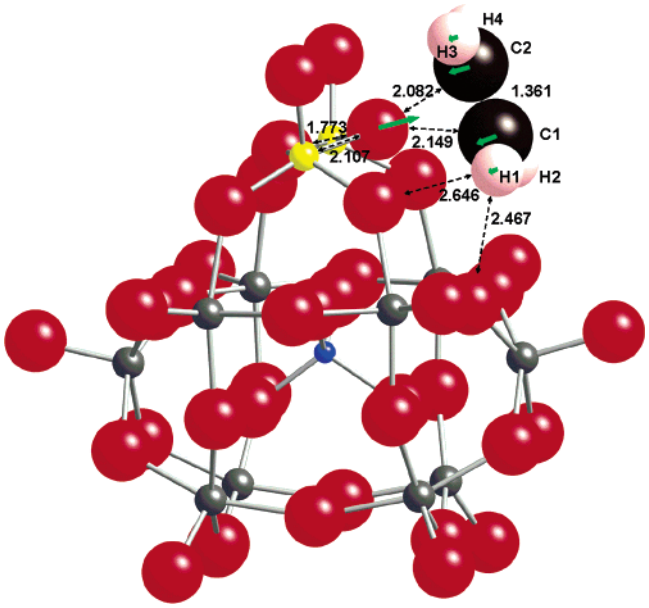

Figure 9. Ball and stick representation for the calculated structure at the transition state of the reaction between **III** and ethene (lengths in Å). Blue, gray, red, yellow, black, and white balls represent silicon, tungsten, oxygen, vanadium, carbon, and hydrogen atoms, respectively. Green arrows show the displacement vectors of the vibration mode with an imaginary frequency. The value of the imaginary frequency is 371*i* cm^{-1}.

([H_2O], Figure 6C). The dependence of the rate on the concentration of 1-octene ([1-octene], 11−100 mM) showed saturation kinetics (Figure 6D). The epoxidation of 1-octene, *cis*-2-octene, and cyclooctene with weak steric effects and different electron densities showed the same time courses at the high substrate concentrations (167 mM) (Figure S8). These dependences can be explained by the change of the rate-determining step from the oxygen transfer step from **III** to the C=C double bond (at low concentration of 1-octene) to the regeneration of **III** (at high concentration of 1-octene).

On the basis of all of the results, we propose a possible reaction mechanism in Scheme 1, which is divided into the following five elementary processes

$$\mathbf{I} + H_2O_2 \xrightarrow{k_1} \mathbf{II} + H_2O \quad (6)$$

$$\mathbf{II} + H_2O \xrightarrow{k_2} \mathbf{I} + H_2O_2 \quad (7)$$

$$\mathbf{II} \xrightarrow{k_3} \mathbf{III} + H_2O \quad (8)$$

$$\mathbf{III} + H_2O \xrightarrow{k_4} \mathbf{II} \quad (9)$$

$$\mathbf{III} + \text{alkene} \xrightarrow{k_5} \mathbf{I} + \text{epoxide} \quad (10)$$

(k_1−k_5: rate constants)

First, the bis-μ-hydroxo compound **I** reacts reversibly with hydrogen peroxide to form the μ-hydroxo-μ-hydroperoxo species of **II** (eqs 6 and 7; step 1). The compound **II** is reversibly dehydrated to form the active oxygen species **III** (eqs 8 and 9; step 2). Then, **III** reacts with alkenes to form the corresponding epoxides (eq 10; step 3). The overall epoxidation rate is expressed by eq 11 (see details in Supporting Information). On the basis of the kinetics and ^{51}V NMR data, the rate constants k_1−k_5 were calculated to be 0.022 mM^{-1} min^{-1}, 0.291 mM^{-1} min^{-1}, 34.2 min^{-1}, 1.69 mM^{-1} min^{-1}, and 12.2 mM^{-1} min^{-1}, respectively (alkene, 1-octene; solvent, MeCN/*t*-BuOH (v/v = 1/1); temp, 293 K). The time course of epoxidation calculated by the numerical integration of eq 11 (shown by the solid lines) fairly well reproduced the experimental results of epoxide yields and [**II**] and [**III**] as a function of time (Figure 7), supporting Scheme 1. The slight deviation of the observed yields from the calculated ones at a longer reaction time is probably explained by the nonproductive decomposition of H_2O_2.

$$\text{rate} = \frac{k_1k_3k_5[\text{catalyst}][H_2O_2][\text{alkene}]}{k_2k_4[H_2O]^2 + (k_2[H_2O] + k_3)k_5[\text{alkene}]} \quad (11)$$

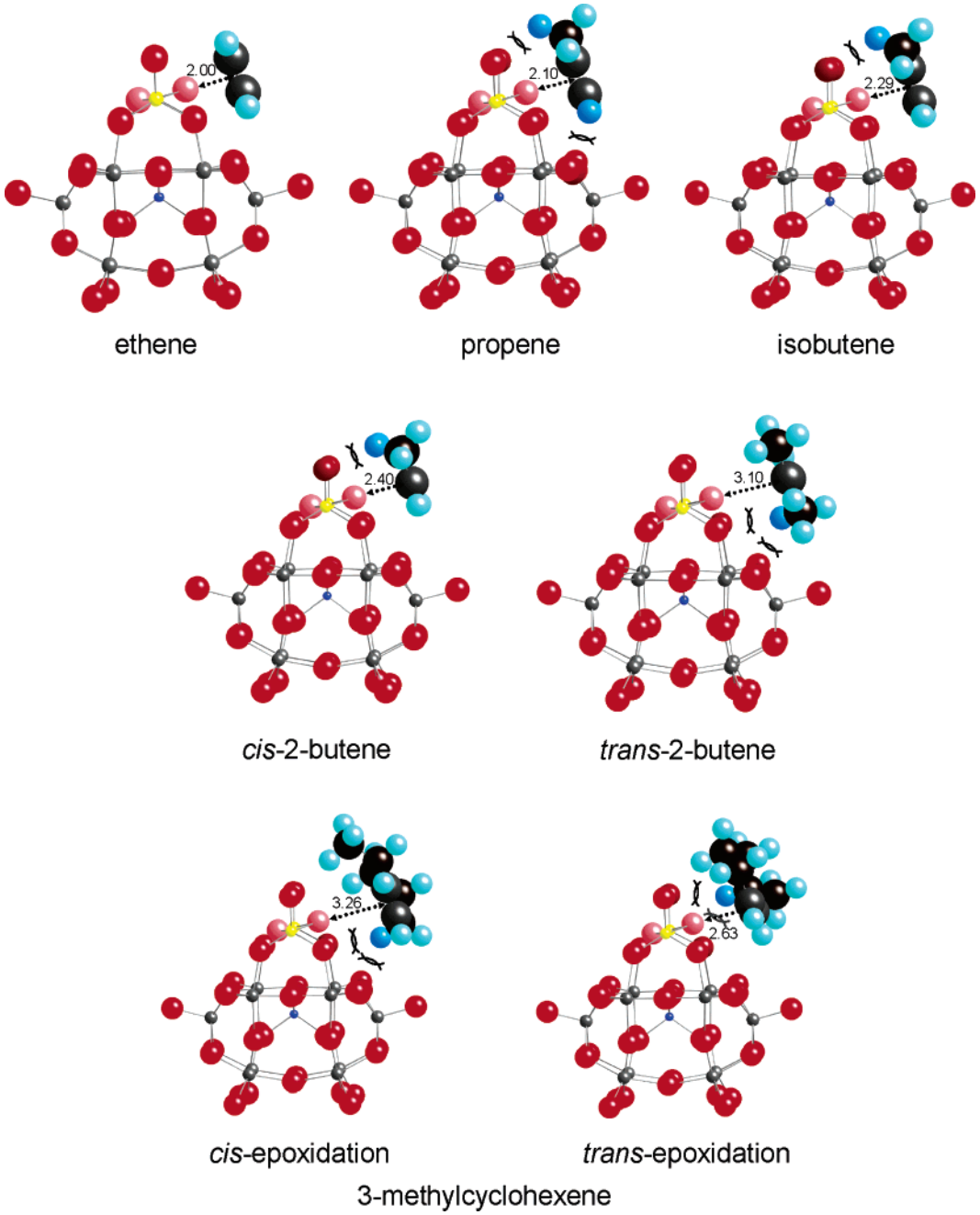

Figure 10. Approaches of various alkenes to **III** (distances in Å).

Quantum Chemical Calculations. The energies of the reaction steps calculated with density functional theory according to Scheme 1 are summarized in Figure 8.[35−40] The calculated reaction energy of step 1 was small (exothermic, −14 kJ mol^{-1}), in agreement with the fact that this step was reversible. The formation of the active complex **III** and H_2O from **II** (step 2) was calculated to be energetically much unfavorable ({E(**III**) + E(H_2O)} − E(**II**) = +71 kJ mol^{-1}), in agreement with the fact that **III** was not formed in aprotic solvents, where the stabilization of H_2O by solvation is

(35) We used ethene as a model substrate for the computational approach to the **I**-catalyzed epoxidation because of the very large system size. The geometry optimization of the transition state of the reaction between **III** and ethene took 3 months with our Intel Xeon 2.8 GHz server computer. The use of ethene as a model substrate is common in the computational study of the alkene epoxidation.[36−39]

(36) Deubel, D. V.; Sundermeyer, J.; Frenking, G. *J. Am. Chem. Soc.* **2000**, *122*, 10101.
(37) Gisdakis, P.; Antonczak, S.; Köstlmeier, S.; Herrmann, W. A.; Rösch, N. *Angew. Chem., Int. Ed.* **1998**, *37*, 2211.
(38) Sever, R. R.; Root, T. W. *J. Phys. Chem. B* **2003**, *107*, 4090.
(39) Quiñonero, D.; Morokuma, K.; Musaev, D. G.; Mas-Ballesté, R.; Que, L., Jr. *J. Am. Chem. Soc.* **2005**, *127*, 6548.

(40) Since all of the polyoxometalates used for the calculations have the same charge of −4 and the sizes are almost the same, the solvent effects on polyoxometalates are probably close to one another. The solvent effects on H_2O_2 and H_2O are probably close to each other since both molecules are neutral and the sizes are almost the same. Thus, the solvent effects would not much affect the reaction energy (−14 kJ mol^{-1} exothermic) of step 1 (**I** + H_2O_2 → **II** + H_2O). In a similar way, the reaction energy (−217 kJ mol^{-1} exothermic) and the energy barrier (+49 kJ mol^{-1}) of the reaction of **III** with ethene (**III** + C_2H_4 → $SiV_2W_{10}O_{39}^{4-}$ + C_2H_4O) would not be much affected by the solvent effects. On the other hand, the reaction energy (71 kJ mol^{-1} endothermic) of step 2 (**II** → **III** + H_2O) would be lowered in polar, protic solvents such as MeCN/*t*-BuOH where H_2O is stabilized.

small.[40] The energy barrier of the oxygen-transfer reaction of **III** with ethene (step 3) was calculated to be 49 kJ mol^{-1}. The value is smaller than those calculated for the epoxidation of ethene with peracetic acid (71 kJ mol^{-1}) and dimethyldioxirane (72 kJ mol^{-1}) at the B3LYP/6-31++G** level and than those reported for molybdenum diperoxo complex $[MoO(O_2)_2(OPMe_3)]$ (69 kJ mol^{-1}),[36] $[CH_3Re(O)(O_2)_2]\cdot H_2O$ (68 kJ mol^{-1}),[37] and titanosilicate model complex $[Ti(OSiH_3)_3(\eta^2\text{-}OOH)]\cdot H_2O$ (57 kJ mol^{-1})[38] at the B3LYP level.

Figure 9 shows the calculated structure at the transition state of the reaction between **III** and ethene. The ethene molecule approached along the O−O peroxo bond axis. The O−O peroxo bond was lengthened from 1.496 (**III**) to 1.773 Å, and the C═C double bond was also lengthened from 1.332 (ethene) to 1.361 Å. The C1(ethene)−O(peroxo) and C2(ethene)−O(peroxo) lengths were 2.149 and 2.082 Å, respectively, and very close to each other, suggesting the concerted approach of the C═C double bond to the active oxygen center. The H1 and H2 atoms were surrounded by the polyoxometalate framework, while the H3 and H4 atoms were not. Next, the steric effects of various alkenes were investigated by the substitution of methyl groups for H1−H4 (Figure 9) to form propene, isobutene, *cis*-2-butene, and *trans*-2-butene. All O−H lengths were kept longer than 2.467 Å (the shortest O−H length in Figure 9) by rotating the alkene molecule on the center of the double bond and lengthening the distance between the peroxidic oxygen and the double bond (for ethene, 2.00 Å). The shortest distances between the peroxidic oxygen and the double bonds under these conditions were 2.10, 2.29, 2.40, and 3.10 Å for propene, isobutene, *cis*-2-butene, and *trans*-2-butene, respectively (Figure 10), showing the strong repulsion between the substituents and the polyoxometalate framework for trans-substituted alkenes. The same analysis was performed for the diastereoselective epoxidation of 3-methylcyclohexene. The structure of 3-methylcyclohexene was separately calculated at the B3LYP/6-31++G** level in the restraint that the C═C length was kept at 1.361 Å. The shortest distances of the peroxidic oxygen and the double bond were 2.63 and 3.26 Å for trans- and cis-epoxidation, respectively, suggesting the strong repulsion for the cis-epoxidation.

Conclusions

The results for the oxidation of 3-alkylcyclohexenes, styrenes, and SSO with hydrogen peroxide catalyzed by **I** show that the strong electrophilic oxidant species with the strong steric hindrance is generated. The ^{51}V NMR and CSI−MS spectra show that the reaction of **I** with hydrogen peroxide leads to the generation of the hydroperoxo species **II**. The successive dehydration of **II** forms **III**, which possibly has an active oxygen species of a $\mu\text{-}\eta^2\text{:}\eta^2$-peroxo group. The kinetic and spectroscopic studies show that the present epoxidation proceeds via **III**. The DFT calculation results support the proposed mechanism and explain the steric hindrance of the active oxygen species.

Acknowledgment. We acknowledge Dr. K. Yamaguchi, Mr. T. Imago, Mr. K. Watanabe (The University of Tokyo), Dr. K. Kamata, and Miss M. Kotani (Japan Science and Technology Agency) for their help with experiments. This work was supported, in part, by the Core Research for Evolutional Science and Technology (CREST) program of Japan Science and Technology Agency, a Grant-in-Aid from the Ministry of Education, Culture, Sports, Science, and Technology of Japan for Scientific Research, and a project of Research and Development Projects for Economic Revitalization: The Project to Design Sustainable Management and Recycling System of Biomass, General and Industrial Wastes.

Supporting Information Available: Rate law derivation for the mechanism in Scheme 1, Tables S1−S6, and Figures S1−S8. This material is available free of charge via the Internet at http://pubs.acs.org.

IC0623258